Signal Processing Approaches to Analyzing Patient Cardiovascular State

by

Ekavali Mishra

Submitted to the Department of Electrical Engineering and Computer Science
in partial fulfillment of the requirements for the degree of

Master of Engineering

at the

MASSACHUSETTS INSTITUTE OF TECHNOLOGY

June 2011

Author .....
Department of Electrical Engineering and Computer Science
May 20, 2011

Certified by .....
George C. Verghese
Professor of Electrical Engineering
Thesis Supervisor

Certified by .....
Thomas Heldt
Research Scientist
Thesis Supervisor

Accepted by .....
Christopher J. Terman
Chairman, Department Committee on Graduate Theses

Signal Processing Approaches to Analyzing Patient Cardiovascular State

by

Ekavali Mishra

Submitted to the Department of Electrical Engineering and Computer Science
on May 20, 2011, in partial fulfillment of the
requirements for the degree of
Master of Engineering

Abstract

There is a wealth of unanalyzed data stored in patient records that could yield insight into a patient's cardiovascular state during surgery and causes of fluctuations in hemodynamics. Recent work suggests that time spent outside a certain blood pressure range corresponds to an increased risk of adverse outcomes after surgery. An analysis of blood pressures recorded during surgery could also be tied to patient fluid responsiveness, pulse pressure variability (PPV) can be a predictor of fluid responsiveness in surgical patients. Thus, a comparison of physiological variables such as cardiac output (CO), total peripheral resistance (TPR), and PPV of patients who experience adverse outcomes to those who do not could help explain the link between adverse outcomes and intraoperative blood pressure variations. Data from patients undergoing cardiothoracic surgery was used to investigate intraoperative hemodynamics. Patients were separated into two groups: those who experienced adverse outcomes within 30 days of surgery (cases) and those who did not (controls). A comparison of blood pressure values extracted from patient data revealed that cases had higher systolic and lower diastolic values during surgery. CO and TPR were computed from these data but a comparison of variability for the two groups yielded no conclusive results.

Thesis Supervisor: George C. Verghese
Title: Professor of Electrical Engineering

Thesis Supervisor: Thomas Heldt
Title: Research Scientist

Acknowledgments

I would like to thank the many people whose continued support and encouragement made this work possible. To Professor George Verghese, starting with 6.011 and continuing this past year, your patience and gentle encouragement have made you a wonderful advisor. Your guidance in pursuing my research showed me how to question my assumptions and I feel very fortunate to have worked under your supervision.

My thesis co-supervisor, Dr. Thomas Heldt, was both a patient mentor and a great teacher. I was frequently awed by his technical knowledge and credit him with teaching me many of the cardiovascular concepts and models I learned this year. His help has been significant in all parts of my work and I thank him for the time he put into my project, especially the many hours of editing.

Thanks to Dr. Balachundhar Subramaniam at Beth Israel Deaconess Medical Center for his interest and support in the project, providing us the patient data used in our analysis.

I also thank the rest of the members of the Computational Physiology and Clinical Inference group – the new Dr. Faisal Kashif for always being supportive, Priya for always smiling, Ankit and Irena for their jokes, and Becky for her cheerful attitude.

Finally, I would like to thank my parents and sister for their positive encouragement and support all through my time at MIT.

Contents

List of Figures

List of Tables

Chapter 1

Introduction

1.1 Monitoring Patient Hemodynamics

Currently, patients admitted to an Intensive Care Unit (ICU) are closely monitored by a number of devices and tests that record and output important data regarding their physiological state. These records come in multiple forms; physiological signals from bedside monitors, records of administered fluids and medications, imaging results and other tests. The variety of sources forces clinicians to spend time processing and interpreting all the data, creating a 'data-overload' problem in which they are forced to recognize trends in clinical data derived from a multitude of sources. This presents the opportunity to integrate the available multi-parameter data and develop a system that can track and analyze a patient's pathophysiologic state, concentrating all information and data analysis in one computer. The involved signals are a collection from the hospital archives and patient bedside networks. Possibilities for such a system include deriving physiological variables based on an analysis of the collected waveforms; this would have the benefit of producing more relevant information in a concentrated source, thereby enabling physicians to make earlier and more accurate diagnoses.

For patients undergoing surgery, such a system can include the hemodynamic variables tracked in the operating room, and can possibly help prevent adverse outcomes after surgery. For instance, studies have shown that blood pressure can be used to predict the likelihood of adverse events during a patient's peri-operative period. Specifically, Aronson *et al.* showed that patients whose intraoperative systolic blood pressure (SBP) varied outside the range of 105 to 130 mm Hg were more likely to experience adverse outcomes within thirty days

of surgery [1]. Figure 1-1 illustrates a similar analysis done by Chen *et al.*, suggesting that SBP excursion outside a range of 75 to 145 mm Hg over a 24-hour window increases risk of adverse outcomes for surgical patients. It is possible to explore the physiological rationale for this difference in blood pressure values by delving into the information collected during surgery. Ranging from records of medications and administered fluids to arterial blood pressure (ABP) and electrocardiogram (ECG) waveforms, the data measured during surgery allow for continuous estimation of signals that can only be measured invasively. Since patients undergoing surgery are often already in a vulnerable state, invasive tests increase the risk of complications after surgery. Continuous values for variables such as cardiac output (CO), the amount of blood pumped by the heart per unit time, and Total Peripheral Resistance (TPR) of the arterial tree, derived from the ABP signal recorded during surgery, can reveal trends during surgery without further endangering a patient's health through invasive measurements. Furthermore, this information allows surgeons and anesthesiologists to make more informed decisions during the surgery and reduce the likelihood of an adverse outcome after surgery.

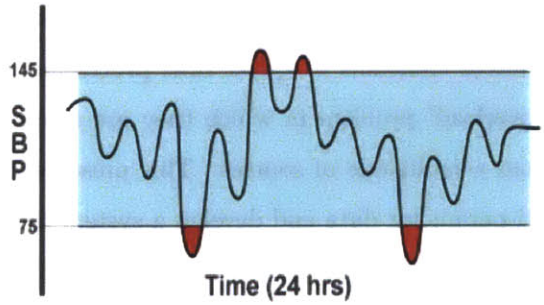

Figure 1-1: Risk of adverse outcomes is proportional to the aggregate excursion outside a certain range for SAP, depicted above as the area shaded in red [2].

1.2 Using Arterial Blood Pressure

There is a wealth of information in the patient data recorded during surgery that can yield further insight into a patient's physiological state. However, using the ABP signal recorded during surgery in an analysis of hemodynamics has multiple advantages. ABP is continuously monitored using a minimally invasive procedure, providing a waveform from which continuous estimates of CO and TPR can be obtained (to within a scale factor).

Extracting CO and TPR estimates from the ABP waveform is a noninvasive procedure and therefore safe and cost-effective. A system that processes the data recorded during surgery could help clinicians identify trends in both monitored variables and derived variables, such as CO and TPR. Additionally, integrating data regarding a patient's cardiovascular state with the records of fluids administered during surgery as well as respiratory rate can provide additional insight into a patient's cardiovascular state and may guide therapy. Thus, we can improve monitoring of surgical patients and further explore cardiovascular dynamics by integrating and analyzing data recorded during surgery, with the ultimate goal of reducing adverse events during and after surgery.

1.3 Specific Aims

Currently, there are several methods of estimating CO and thus TPR from the ABP waveform. This work seeks to compare these methods of estimation for patients undergoing surgery. The estimated waveforms can also help towards understanding trends in the data, thereby supplying clinicians with more information about a patient's state. Ultimately, this additional insight could help differentiate between patients who experience adverse events after surgery and those who do not.

As mentioned, an analysis of the cardiovascular state of a patient undergoing surgery includes integrating the different records kept during surgery. Because changes in hydration status have effects on pulse pressure and thus fluid responsiveness in critically ill patients, we also will analyze the pulse pressure time series (obtained from the ABP signal) [9]. Thus, the analysis of CO and TPR can include information noted in a separate record from the ABP signal, such as the ventilator rate and fluids administered for a patient under surgery. This is a step towards integrating data from separate sources in an effort to explore cardiovascular dynamics.

The aims of this thesis are:

1. To compare and validate methods of estimation for cardiovascular variables including Cardiac Output and Total Peripheral Resistance for patients undergoing surgery.

2. To identify trends in the estimated values for these variables.

3. To identify trends in cardiovascular dynamics related to respiration by integrating data

from the arterial blood pressure waveform with the records for respiratory frequency and fluid administration during surgery.

1.4 Outline

This thesis is organized in five chapters. In Chapter 2, we will review the relevant elements of cardiovascular and respiratory physiology. In Chapter 3, we describe the basis of several algorithms for estimation of cardiac output and total peripheral resistance. Chapter 4 shows and explains the results obtained by analyzing patient blood pressure signals to differentiate between patients who experience adverse outcomes after surgery and those who do not. Chapter 5 concludes this thesis with a summary of my work and an explanation of future work.

Chapter 2

Cardiovascular and Respiratory Physiology

2.1 Functional Anatomy of the Heart

The cardiovascular system is responsible for the transport of blood throughout the body and thus both the delivery of oxygen and nutrients to the body's organs, and the removal of waste and carbon dioxide from the organs. It includes the heart, which pumps blood to the organs, and blood vessels of various sizes, which carry blood through the body.

Blood vessels fall in three main categories: arteries, veins, and capillaries. Arteries are the largest of the three and carry blood away from the heart. They have thick walls because they are under the highest amount of pressure of any vessel in the vasculature. The arteries branch into smaller arterioles that feed into the capillaries, the site of gas and nutrient exchange in the organs. The veins are thin-walled structures that store the largest amount of blood in the cardiovascular system and carry blood back to the heart [3] . Blood vessels impede the flow of blood through the body; the aggregate resistance of the peripheral (or systemic) vasculature is termed the Total Peripheral Resistance (TPR).

The heart functions as two pumps, each comprising an atrium and a ventricle. The atria are connected to the ventricles via the atrioventricular valves, which prevent blood from flowing backwards through the heart. The right heart pumps deoxygenated blood through the pulmonic valve into the pulmonary artery. From here, blood flows through the pulmonic circulation of the lungs, where gas exchange occurs. The left heart pumps the

oxygenated blood from the pulmonic system through the aortic valve and into the aorta. From the aorta, blood is directed to the body's organs through the systemic circulation. The two pumps of the heart function in series; blood travels through the right heart and through the pulmonary circulation to the left heart, which pumps it through the systemic circulation before it returns to the right heart.

2.2 The Cardiac Cycle

The cardiac cycle refers to the sequence of events relating to the flow of blood through the heart during a single heartbeat. As depicted in Figure 2-1, the cardiac cycle begins with atrial systole, when the atria both contract. Next, the ventricles contract, increasing their pressure; once the pressures in the ventricles exceed the pressures in the atria, the atrioventricular valves (mitral and tricuspid valves) close. The ensuing phase is termed isovolumic contraction – the ventricles continue to contract after the atrioventricular valves close, increasing the pressure in the ventricles although the volume remains constant. The semilunar valves (aortic and pulmonic valves) open when the pressures in the ventricles exceed the pressure in the aorta (for the left ventricle) and pulmonary artery (for the right ventricle). The pressure increases to a maximum value, creating a pressure gradient and ejecting blood from the ventricles. At the same time, the atria are filling with blood in preparation for the next cardiac cycle. Ventricular pressures and volumes decrease as blood leaves the chambers; once pressures dip below that of the aorta and pulmonary arteries, respectively, the semilunar valves close and the ventricles relax. During the ensuing isovolumic relaxation phase, the pressures decrease and volumes remain constant. The atrioventricular valves open once ventricular pressures dip below atrial pressures, commencing ventricular filling and the last stage of the cardiac cycle.

The cardiac cycle can be separated into two parts: diastole and systole, both of which can be extracted from the arterial blood pressure waveform. Diastole corresponds to isovolumetric relaxation and ventricular filling, while systole corresponds to the phase of ventricular contraction, comprising isovolumic contraction and ejection. On the arterial blood pressure waveform, the diastolic arterial blood pressure (DAP) is the minimum, roughly the pressure at the time the aortic valve opens. The systolic arterial blood pressure (SAP) is the maximum, occurring prior to the closing of the aortic valve.

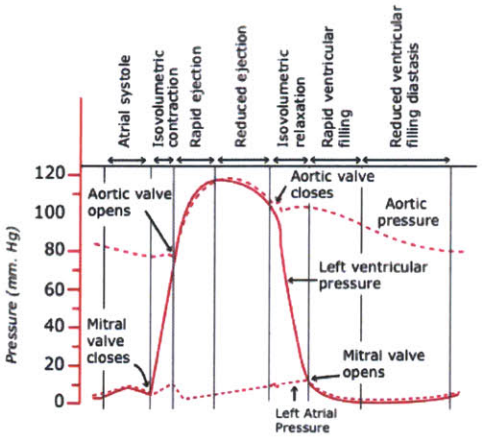

Figure 2-1: Pressure waveforms in the left atrium, left ventricle, and aorta corresponding to each phase of the cardiac cycle [10].

2.3 Pressure and Volume in the Ventricles

The ventricles are composed of myocardial cells that form muscle fibers. These fibers control the pressure and volume of the ventricle, determining the amount of blood that can be stored during systole and diastole. Pressure in the ventricle is dependent on the tension developed in the myocardial cells. This tension varies with the length of the fiber, which in turn affects the volume of the ventricle. The preload, defined variably as the end-diastolic volume (EDV) or the end-diastolic pressure (EDP), is related to the end-diastolic length of the muscle fibers. It is possible to draw a relation between the preload and pressure developed in the ventricle or output delivered by the ventricle during systole. The development of pressure in the ventricle during systole is an active mechanism, as opposed to during diastole, when the pressure increases passively with volume. As a result, there is a different relation between pressure and volume in the ventricle during systole and diastole. Figure 2-2 illustrates the ventricular pressure-volume curves, which represent the compliance characteristics of the ventricle. At point 1, pressure in the ventricle is equal to the filling, or preload, pressure. The mitral valve closes and the ventricle begins to contract (isovolumetric contraction). Systole begins when the aortic valve opens, at point 2, after pressure in the ventricle exceeds pressure in the aorta at the diastolic pressure (DAP). As blood is ejected from the ventricle into the aorta, pressure in both increases to the systolic pressure (SAP) at point 3, and then decreases as the ventricle empties. The aortic valve

closes at point 4, when pressure in the ventricles is equal to the aortic or afterload pressure, and the ventricle relaxes (isovolumetric relaxation). At point 5, pressure in the ventricle is the same as pressure in the atrium and the mitral valve opens, initiating diastole and filling of the ventricle

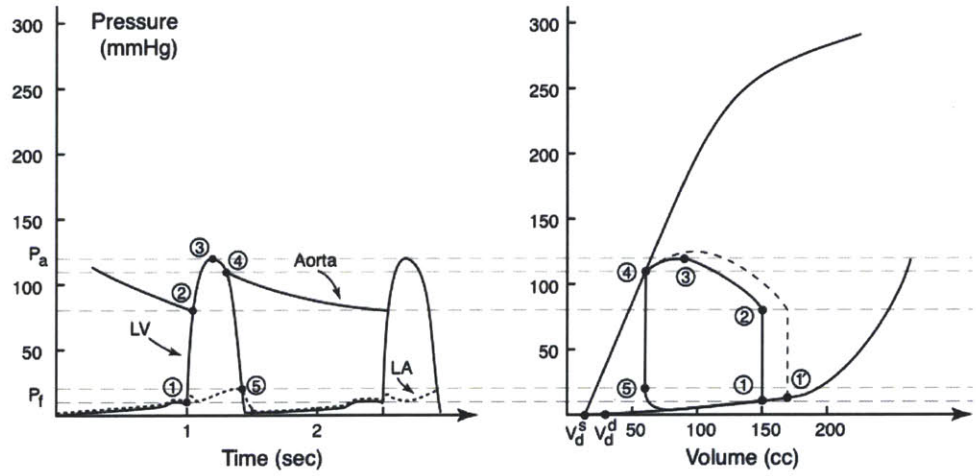

Figure 2-2: Pressure-time (left) and pressure-volume (right) relationships in the left ventricle (see text for details) [10].

This relation between pressure and volume in the ventricles is known as the Frank-Starling mechanism, and states that – within limits – the output from the heart increases as preload increases. As noted in Figure 2-3, the Frank-Starling relationship between preload and SV is curvilinear, showing that the compliance varies with the preload.

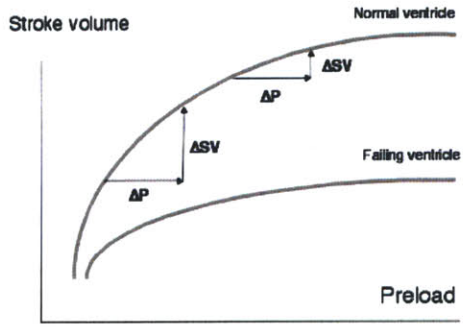

Figure 2-3: The Frank-Starling relationship of the heart indicates the extent to which fluctuations in stroke volume correspond to fluctuations in the preload (also known as atrial or filling pressure) [11].

2.4 Cardiac Output

The cardiac output (CO) is the rate at which blood is pumped out of either ventricle, and is an important indicator of a patient's hemodynamic state. It is closely related to the stroke volume (SV), the amount of blood ejected by a ventricle per heartbeat. Given that the end-diastolic volume (EDV) is the volume in the ventricle before it contracts, and the end-systolic volume (ESV) is the volume after contraction, then

$$SV = EDV - ESV \tag{2.1}$$

Using heart rate, HR, one can then calculate CO using

$$CO = HR \cdot SV \tag{2.2}$$

For a normal adult at rest, CO is approximately 6 L/min, HR is about 70-80 beats/min (bpm), and SV is approximately 80 mL/beat.

There are several methods of directly measuring cardiac output, including an ultrasonic flowmeter, the Fick Principle, thermodilution, and ultrasonography. Currently, thermodilution is the method most commonly used to assess CO in clinical settings like the operating room or intensive care units.

A flowmeter is an ultrasonic flow probe that is placed around the ascending aorta and measures instantaneous flow in the aorta. Stroke volume is then the flow waveform integrated over the cardiac cycle, and as previously discussed, CO is the product of heart rate and stroke volume, or the time-average of the flowmeter waveform. This technique requires opening of the chest in order to place a flowmeter around the aorta, rendering it an invasive procedure that is most often used in animal experiments rather than human patients.

The Fick Principle uses the idea of mass balance applied to oxygen consumption. The amount of oxygen consumed per unit time is equal to the difference of oxygen concentration in the arteries and oxygen concentration in the veins, multiplied by CO. Thus

$$\text{CO} = \frac{\text{O}_2 \text{ consumed per unit time}}{\text{arterial } [\text{O}_2] - \text{mixed venous } [\text{O}_2]} \tag{2.3}$$

However, a blood sample from the pulmonary artery is required in order to measure mixed-venous oxygen content, making this an invasive technique as well.

Thermodilution also involves the pulmonary artery: a bolus of cold saline is injected in the the pulmonary artery and the temperature is measured downstream in order to obtain the rate of change in temperature. Cardiac output can be obtained from the integral of the temperature waveform. As mentioned, thermodilution is the method most commonly used in clinical settings to obtain CO, despite being highly invasive.

Ultrasonography measures the velocity of blood through the aorta. If A is the cross sectional area of the aorta, T is the length of a cardiac cycle, and $v(t)$ is the blood flow velocity, then:

$$SV = A \int_T v(t)dt \tag{2.4}$$

and

$$CO = HR \cdot A \int_T v(t)dt \tag{2.5}$$

Impedance cardiography is also known as electrical impedance plethysmography, and uses sensors on the neck and chest to detect the resistive properties of blood flow in the thorax. This information is then used to calculate values for hemodynamics. Although noninvasive, this method requires expensive equipment.

M-mode scanning or 4D Imaging is another noninvasive method of calculating cardiac output. However, as with impedance cardiography, it requires expensive equipment.

Most of the current methods of measuring cardiac output, although reasonably accurate, have several disadvantages. Many require invasive procedures that pose a risk to patients, especially those who are already critically ill, while noninvasive methods are generally expensive. Others require expensive capital equipment or access to an expert technician or clinician. Furthermore, these methods do not allow for continuous measurement of CO. In Chapter 3, we will discuss how CO can be derived from the ABP waveform.

2.5 Fluid Responsiveness

Changes in total blood volume (TBV), although a small percentage of overall fluid in the body, can have a large influence on ABP and CO. Often, critically ill patients are loaded with fluids in order to increase SV, thus increasing CO and ABP. When fluid is administered, filling pressure increases. If the patient already operates on the flat portion of the Frank-Starling curve (see Figure 2-3), then SV might not increase by much. At higher filling pressures, the Frank-Starling curve levels off, meaning that changes in the preload correspond to minimal changes in SV. Further increasing the preload will increase the stress on the heart, which can be very detrimental in patients with weak hearts. Fluid responsiveness is then defined as the amount of change in SV as a result of changes in preload.

Patients undergoing surgery are often placed on mechanical ventilation, causing periodic respiratory shifts in SV due to ventilator-induced changes in intra-thoracic pressure. The magnitude of the shifts in SV can then be used to asses fluid responsiveness. During inspiration, positive pressure ventilation decreases the pressure gradient for blood returning to the heart (venous return) thus decreasing right-ventricular preload. Inspiration also increases right-ventricular afterload by increasing intrathoracic pressure. As a result, during inspiration, filling pressure, and thus SV, decreases. During exhalation, filling pressure increases, thus increasing stroke volume. Pulse pressure (PP) is the difference between SAP and DAP and a surrogate for SV, as will be made clear in Chapter 3. Michard and Teboul [12] have shown that PP variability (PPV) over each respiratory cycle is a predictor of fluid responsiveness in patients. Patients with a low PPV were found to respond poorly to volume expansion (administration of fluids), whereas patients with a higher PPV were more responsive to volume expansion [12]. The authors defined PPV as

$$\mathrm{PPV} = 100\% \times \frac{\mathrm{PP}_{max} - \mathrm{PP}_{min}}{(\mathrm{PP}_{max} + \mathrm{PP}_{min})/2} \tag{2.6}$$

where PP_{max} and PP_{min} are the maximum and minimum PP over a single respiratory cycle, as shown in the figure below.

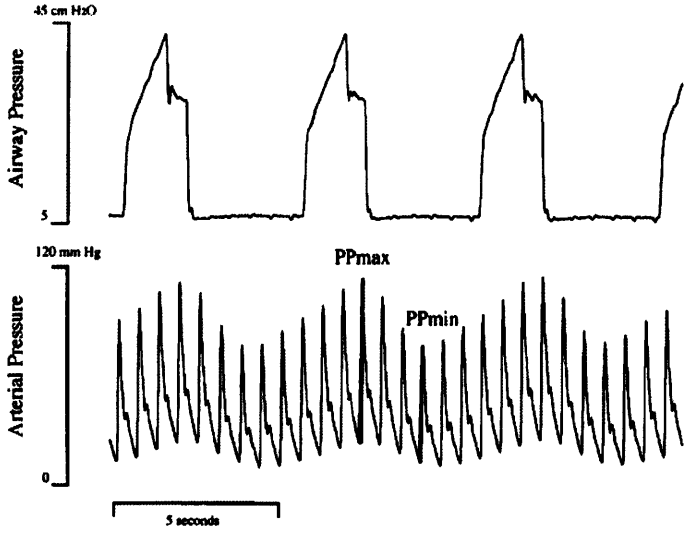

Figure 2-4: Respiratory changes in airway pressure (top) and arterial pressure (bottom) for a mechanically ventilated patient. PP is at a maximum as the end of inspiration, while the minimum PP is recorded during expiration [12].

2.6 Medications Administered During Surgery

What follows is a list of the drugs administered to the patients studied during surgery. These drugs are given in response to a patient's physiological state and often affect intraoperative hemodynamics, causing shifts in ABP, CO, and TPR. As a result, it is helpful to take these medications into account in order to gain a more thorough understanding of these physiological variables.

Cefazolin is used to treat bacterial infections.

Dexmedetomidine is a sedative that depresses cardiovascular responses in the perioperative period. It is used as a short-term sedative and slightly decreases sympathetic tone, thus reducing heart rate and blood pressure.

Esmolol inhibits the effects of epinephrine and norepinephrine, decreasing contractility of the heart and heart rate. It is characterized by a rapid onset and short duration.

Etomidate is a short-acting (5-10 minutes) anesthetic that allows for conscious sedation and is less likely to cause a drop in blood pressure compared to other general anes-

thetics.

Fentanyl relieves pain, falling under the opiate class of analgesics. Its effects are characterized by a rapid onset and short duration.

Heparin is an anticoagulant that helps prevent blood clots from forming.

Hydrocortisone raises blood pressure by increasing the vasculature's sensitivity to epinephrine and norepinephrine.

Lydocaine is a local anesthetic characterized by a rapid onset. It prevents pain by blocking the propagation of pain signals and is sometimes associated with hypotension when combined with general anesthesia.

Midazolam is used in conjunction with Fentanyl before anesthesia. It also has a short duration and can cause hypotension if given too fast.

Nitroglycerine relaxes blood vessels in the peripheral vasculature, reducing the strain on the heart to pump oxygen to the body. Dilation of the blood vessels lowers total peripheral resistance and arterial blood pressure.

Pancuronium is a muscle relaxant used with anesthesia to aid mechanical ventilation during intubation. It slightly reduces activity of the vagus nerve, moderately increasing heart rate and thus blood pressure.

Phenylephrine is a vasoconstrictor commonly used as a nasal decongestant because it constricts the nasal blood vessels and decreases blood flow to the sinus vessels. In surgery, it is administered to increase blood pressure without affecting heart rate or contractility.

Propofol is an anesthetic that inhibits sympathetic stimulation, thus inducing vasodilation and leading to low blood pressure.

Protamine is used in cardiopulmonary bypass surgery to rapidly reverse the anticoagulant effects of heparin. The interaction between protamine and heparin has been shown to cause increased pressure in the pulmonary artery and decreased cardiac output, arterial pressure, heart rate and vascular resistance.

Succinycholine is a short-term paralytic and muscle relaxant, often administered during surgery to aid with tracheal intubation.

Tranexamic Acid reduces blood loss by inhibiting the destruction of fibrin, an important component of blood clots. Specifically, it inhibits the production of plasmin, which degrades fibrin and thus prevents the formation of blood clots.

Vancomycin kills bacteria and is a drug of last resort in order to prevent the development of resistant bacteria.

Chapter 3

Models of Cardiovascular Dynamics

Models of the cardiovascular system can help interpret experimental results or clinical data and can be used to estimate physiological variables that cannot or are usually not measured directly. In this sense, they might help provide a more comprehensive understanding of hemodynamics. In this chapter, we go through the models used in our CO analysis of surgical patients. There are currently a number of models in use, some of which can be framed as electrical circuit analogs, modeling components of the vasculature as resistive and capacitive elements. In Section 3.1, we introduce the notion of a lumped-parameter model of the circulation. In Section 3.2, we describe the well-known Windkessel model, which underlies several of the methods for CO estimation from the arterial blood pressure waveform (so called pulse-contour methods). In Section 3.3, we review several pulse-contour methods for CO.

Table 3.1: Cardiovascular variables and the corresponding electric circuit analogs. Adapted from [10].

Cardiovascular Variable	**Electrical Variable**
Pressure, P	Voltage, v
Flow, Q	Current, i
Volume, V	Charge, q
Resistance, $R = \Delta P/Q$	Resistance, $R = \Delta v/i$
Capacitance, $C = \Delta V/\Delta P$	Capacitance, $C = \Delta q/\Delta v$

3.1 Lumped-Parameter Model

As blood flows through the body, blood vessels pose resistance to the flow. Equation 3.1 describes the relationship between pressure, P, in the vessel and blood flow, Q, through the vessel, assuming that the vessel wall is rigid and the flow is steady (i.e. non-pulsatile), laminar, and blood is a Newtonian fluid.

$$\Delta P = QR \tag{3.1}$$

Thus, resistance is a constant that describes the linear relationship between the pressure difference along the vessel, ΔP, and flow through the vessel. This constant of proportionality, the resistance R, is dependent on the radius, r, of the vessel, the viscosity of blood, μ, in the vessel, and the length, l, of the vessel:

$$R = \mu \frac{8l}{\pi r^4} \tag{3.2}$$

There are many more of these high-resistance paths in parallel, so the effective resistance could be small. In the end, the arterioles contribute the most to resistance (because they individually have high resistance, and there aren't enough of them for the parallel combination to counter that). The arterioles also are the most controllable part of the resistance. The factor of r^4 in the denominator suggests that the smaller vessels, including the arterioles and capillaries, contribute most to the overall resistance of the vasculature. Units of resistance, assuming pressure is in mmHg and flow is measured in mL/sec, are expressed as Peripheral Resistance Units, or PRU. A pressure drop of 80 mmHg and a CO of 5 L/min correspond to a resistance of roughly 1 PRU (mm Hg $\cdot$ sec/ mL).

This model of resistance is dependent on several assumptions regarding the fluid in the vessel and the geometry of the tube and thus does not strictly apply in most vessels of the body. Although these assumptions do not always hold, this model nevertheless serves as a reasonable approximation for the relationship between pressure and flow in the smaller vessels, where most of the cardiovascular system's resistance resides.

Because vessel walls stretch or constrict in response to pressure, vessels have a capacitive quality. If transmural pressure is applied across a vessel, the vessel walls stretch to increase volume and store more blood. As Equation 3.3 demonstrates, the larger the amount of

volume that can be stored in response to a unit step in transmural pressure, the larger the capacitance, C. Certain vessels will stretch more than others depending on the types of cells lining their walls. Vessel walls are composed of an endothelial lining, elastin fibers, collagen fibers, and smooth muscle. Elastin fibers are the most elastic of these four, whereas collagen fibers are the stiffest. The venous system accommodates a much larger fraction of total blood volume than the arterial bed. Furthermore, its pressure-volume relationship is approximately linear over a wide range of distending pressures, and its slope (the incremental compliance) is much larger than that of the arterial tree [6].

$$C = \frac{\Delta V}{\Delta P} \tag{3.3}$$

Figure 3-1 shows the general Lumped-Parameter Model of the peripheral circulation. Blood is pumped from the heart, which is not shown, but which provides the flow, Q. Both the veins and arteries have resistive and capacitive components although, as mentioned before, the resistance of the arterioles dominates the total resistance of the vasculature, and the capacitance of the veins dominates the total capacitance of the vasculature. Table 3.2 shows typical values for the parameters of the model in Figure 3-1.

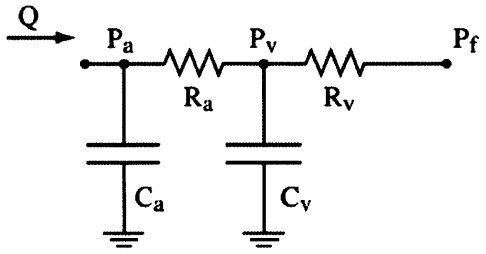

Figure 3-1: Lumped Parameter model of the cardiovascular system, where Q is blood flow, P_a is the arterial transmural pressure, P_v is the venous transmural pressure, P_f is the right atrial (filling) pressure, C_a is the total capacitance of the arteries, C_v is the total capacitance of the veins, R_a is the TPR, and R_v is the resistance to venous flow [10].

3.2 The Windkessel Model

The Windkessel Model simplifies the more general model of the peripheral circulation shown in Figure 3-1. Since the venous capacitance, C_v, is so much larger than the arterial capacitance C_a, fluctuations in venous pressure P_v, are negligible compared to the fluctuations in

Table 3.2: Representative Values for the Lumped Parameter model, adapted from [10].

Variable	Value
C_a	2 mL/mmHg
C_v	100 mL/mmHg
R_a	1 mmHg/mL/sec
R_v	0.06 mmHg/mL/sec

arterial pressure. Thus, it seems justified to replace the venous side of the model by a fixed voltage, representing the filling pressure P_f. However, P_f is essentially 0 mm Hg under normal operating conditions of the cardiovascular system, and so is the pressure outside a large portion of the arterial vessels, which allows us to connect the arterial resistance, R_a, and the arterial compliance, C_a to the same potential, namely ground. Thus, we arrive at the circuit model of Figure 3-2, which is the Windkessel Model, usually attributed to Otto Frank [4, 16] who published on it in 1899. The model describes the lumped resistive and capacitive properties of the arterial tree. Flow is usually modeled as an impulse train, representing pulsatile ejection of blood from the heart into the arteries (see Figure 3-2).

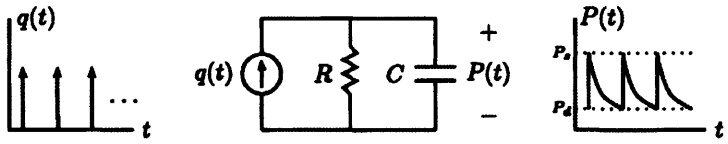

Figure 3-2: Windkessel model of the cardiovascular system. The heart is represented as a current source generating a periodic impulse train, as shown on the left. R and C are the lumped resistive and capacitive components of the arteries, and $P(t)$ is the arterial pressure, where P_s and P_d are SAP and DAP, respectively [17].

In this case, MAP (P_m) is the time-averaged ABP over a single cardiac cycle of period T:

$$P_m = \frac{1}{T}\int_T P(t)dt \tag{3.4}$$

Stroke volume, SV, is given by

$$SV = C_a \cdot PP \tag{3.5}$$

where

$$PP = P_s - P_d \tag{3.6}$$

This results in a convenient expression for CO, since $CO = HR \cdot SV$ and thus,

$$CO = C_a \cdot PP \cdot HR \tag{3.7}$$

As PP and HR can both be directly measured from the ABP waveform, CO can be tracked on a beat-by-beat basis to within a scale factor (C_a) from the the ABP waveform. A single calibration measurement of CO would allow us to determine the constant of proportionality and thus anchor the estimates to provide absolute estimates of CO. Usually it is preferable to have more than one calibration measurement to guard against noise and to provide more robust estimates of CO. In the absence of calibration measurements, Equation 3.7 can still be used to track relative changes in CO (to within the validity of the Windkessel approximation). From an estimate of CO and the available ABP waveform, one can compute an estimate of TPR according to Equation 3.1, namely

$$TPR = \frac{P_m}{CO} \tag{3.8}$$

where it is assumed that venous pressure is zero. An alternative method of obtaining CO using the Windkessel method utilizes the RC time constant, τ of the system:

$$CO = \frac{P_m}{R} = C_a \cdot \frac{P_m}{RC_a} = C_a \cdot \frac{P_m}{\tau} \tag{3.9}$$

If CO is calibrated, TPR estimates according to Equation 3.8 will also provide absolute estimates of peripheral resistance. Many CO and TPR estimation algorithms are derived from variants of the simple Windkessel model. We will describe some of them briefly in the next section.

3.3 Pulse-Contour Methods

The following methods can be used to estimate CO from ABP recordings and were used in our analysis of patient hemodynamics.

The Liljestrand and Zander model [8, 17] modifies the capacitor representing arterial compliance in the Windkessel model. Because arterial compliance varies with pressure – the arteries become stiffer and less compliant as pressure increases – the capacitor is modeled

as a nonlinear compliance. The corresponding CO equation is taken to be

Thus,

$$CO = \frac{k}{P_s + P_d} \cdot PP \cdot HR \tag{3.10}$$

Here, the constant of proportionality, k, is no longer C_a, but a constant with the units of mL/(mm Hg)^2. In our analysis, we tested two different values of k such that the uncalibrated estimates of CO were

$$CO = \frac{P_m - P_d}{P_s + P_d} \cdot HR \tag{3.11}$$

and

$$CO = \frac{P_s - P_d}{P_m + P_d} \cdot HR \tag{3.12}$$

Parlikar [14] describes a method that extracts the beat-to-beat change in onset pressure ΔP, the time-average pressure over each beat $\bar{P}_n$, R and C from each beat. These values are then used to estimate CO for each beat n:

$$CO_n = C_n(\frac{\Delta P_n}{T_n} + \frac{\bar{P}_n}{\tau_n}) \tag{3.13}$$

where the time constant τ_n is estimated from the ABP signal, T_n is the period of each heart beat, and the compliance, C_n can be determined from calibration measurements. Neglecting the term $\frac{\Delta P_n}{T_n}$ yields an alternative estimate, where P_m can approximate ΔP_n:

$$CO_n = C_n(\frac{\Delta P_n}{T_n}) \tag{3.14}$$

The method defined by Herd [7, 13] defines the pulse pressure for each beat, PP_n, as

$$PP_n = \alpha(P_{m,n} - P_{d,n}) \tag{3.15}$$

where $P_{m,n}$ and $P_{d,n}$ are respectively the mean and diastolic pressures for the n^{th} beat. An uncalibrated CO_n estimate is then

$$CO_n = \frac{P_{m,n} - P_{d,n}}{T_n} \tag{3.16}$$

In clinical settings, MAP is a signal that is most easily accessible, as it is often recorded and displayed on a bedside monitor. As a result, CO estimates that replace PP with MAP

are more convenient in some cases. Equation 3.8 shows that if peripheral resistance is constant, MAP is a scaled estimator of CO. However, in the clinical setting, peripheral resistance is only constant in the case that a patient's vasculature is maximally constricted and thus the resistance can change no more. In this case, an uncalibrated estimate of CO is simply

$$CO = P_m \tag{3.17}$$

In the next chapter, we will present the results of applying these estimation algorithms to the data from patients undergoing cardiothoracic surgery.

Chapter 4

Results

In this chapter, we review the results of our explorations. In Section 4.1, we describe the patient data available for our analysis. In Section 4.2, we explain the rationale behind our initial analysis of the data extracted directly from the ABP waveforms recorded during surgery. Section 4.3 further investigates the results of the exploratory analysis described in the previous section by applying the CO estimators described in Chapter 3 to the data to obtain CO and TPR estimates. Finally, Section 4.4 documents the initial steps of analyzing hemodynamics by using PPV and fluid administration during surgery.

4.1 Patient Data

Patient data were obtained from Beth Israel Deaconess Medical Center's Department of Anesthesia, Critical Care and Pain Medicine, where they were recorded during cardiothoracic surgery and streamed to a Philips-designed database server. Patient signals were sampled at 125 Hz with 10-bit amplitude resolution. Records had an average length of 4.5 hours, including about 1.5 hours of non-pulsatile ABP data corresponding to when patients were placed on bypass. Our analysis only involved pre- and post-bypass ABP signals, beginning when the patient was placed on anesthesia. The main pathologies included Coronary Artery Disease (CAD), aortic stenosis, and mitral regurgitation for 10 females and 19 males undergoing Coronary Artery Bypass Graft (CABG) and/or valve replacement procedures. The average age was 68 years for both males and females, with a range of 40 to 84 for women and 43 to 89 for men. Surgical records included medication and fluids administered during surgery and were used in the analysis. Figure 4-1 shows the pulse pressure waveform

of a particular patient. Labeled in the figure are also information from the surgical record, including medications. Signals recorded during surgery usually included arterial blood pressure, pulmonary artery and central venous pressure measurements, three ECG projections, the pulse plethysmogram, and carbon dioxide level – Figure 4-2 gives a snapshot of the signals recorded during surgery.

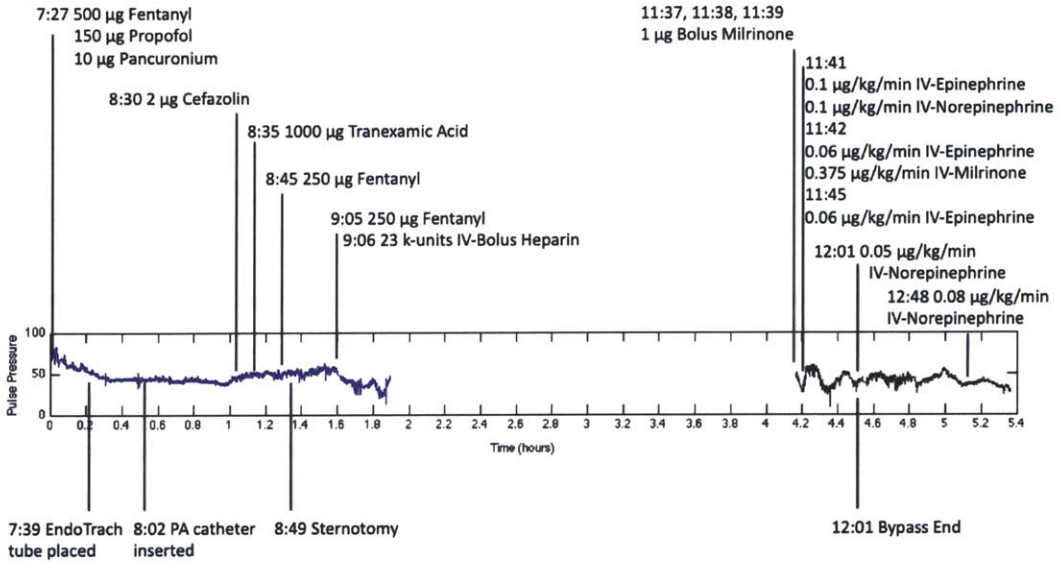

Figure 4-1: Example of patient data recorded during surgery, showing the pulse pressure waveform in terms of time (in hours) for a patient undergoing surgery. The signal is labeled with additional data from the surgical record, including medications administered during surgery and procedures, such as placement of the endotracheal tube to intubate the patient (noted as 'EndoTrach tube placed'), insertion of a catheter in the pulmonary artery (noted as 'PA catheter inserted'), first major chest incision and opening of the chest wall ('Sternotomy'), and the start and end of bypass. ABP is not shown during bypass.

Patients were sorted into two groups; those who experienced an adverse outcome within 30 days of surgery (cases) and those who did not (controls). There were 13 patients in the group of cases and 16 in the control group. After completion of the surgery, the data were retrieved and converted into an open-source Waveform Database (WFDB) format using a custom-made conversion script [5]. An open-source software algorithm was applied to detect the onset of each ABP wavelet [18, 19]. The algorithm is based on the curve length of the ABP waveform and aims to identify the beginning of the systolic upstroke for each ABP wavelet. Records were reviewed for obvious artifacts in the raw data and possible misplaced annotations. These artifacts were given a specific annotation (see Figure 4-3) and were not

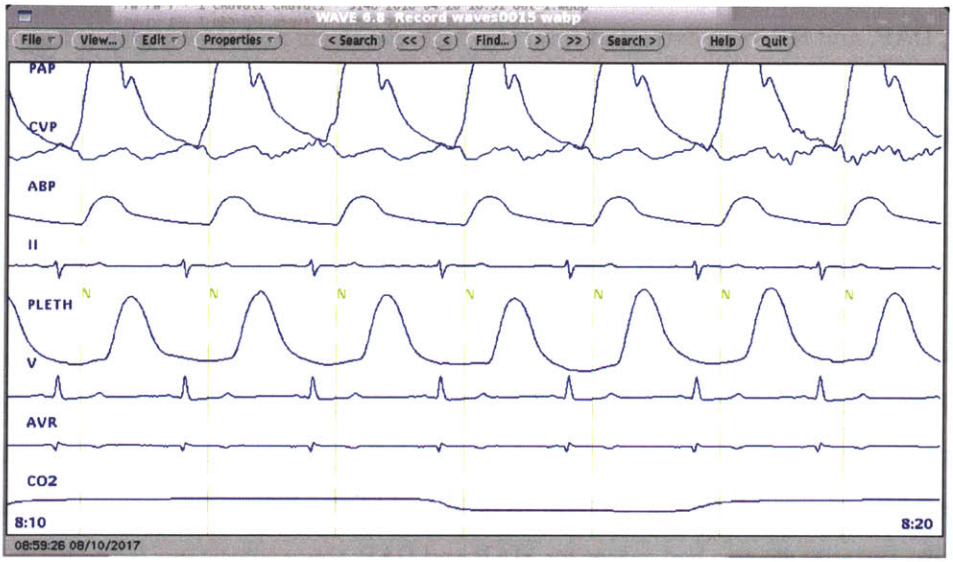

Figure 4-2: An annotated sample of signals collected from the patient database including pulmonary artery pressure (PAP), central venous pressure (CVP), arterial blood pressure (ABP), several ECG projections (I, II, AVR), the pulse plethysmogram (Pleth), and carbon dioxide (CO_2) level waveforms. [N] is the annotation for a normal beat and is marked at the onset of each wavelet. The window corresponds to a 10-second segment of a patients record – the start and end times for this segment are displayed at the bottom corners.

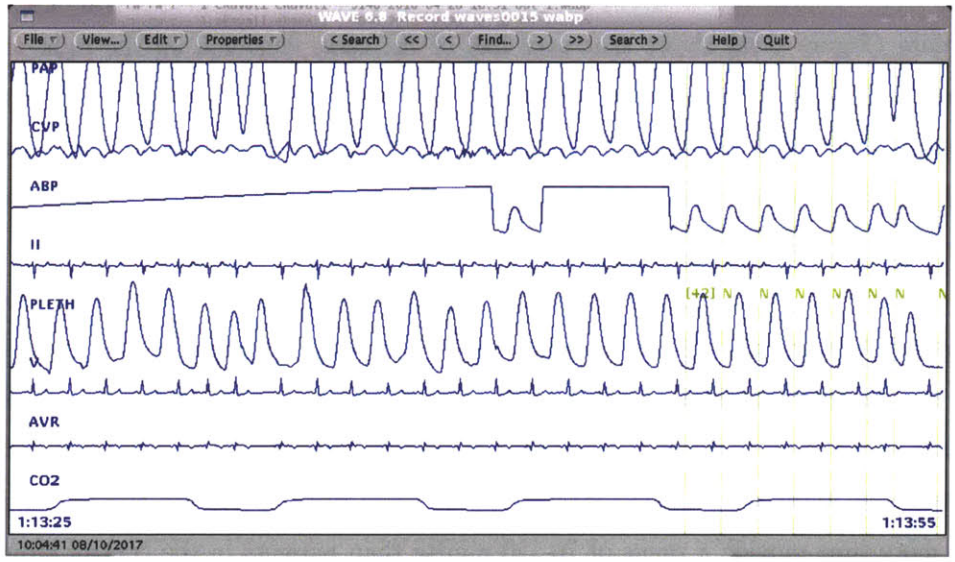

Figure 4-3: The same record as Figure 4-2 but with a larger time interval to show the artifact in more detail (a 30-second time window). Artifacts were given a special annotation [42] and were not included in the analysis of the record.

included in further data analysis. Using these annotations, beat-by-beat numerics of SAP, MAP, DAP, and HR were extracted from the ABP waveform and stored with a time stamp marking the onset of each pulse. The extracted signals were all passed through a 5-point median filter before being analyzed.

4.2 Exploratory Data Analysis

An initial analysis focused on the data directly extracted from the ABP waveform in order to validate findings in the literature and justify a more in-depth investigation. Aronson *et al.* [1] identified excursion limits for SAP during CABG surgery, suggesting that a histogram of the SAP extracted from our surgical records could help differentiate between cases and controls. Because we also had values for MAP and DAP, this analysis was extended to those signals as well. We calculated the cumulative distribution function (CDF) for SAP, MAP, and DAP as seen in Figures 4-4 and 4-5. For a given ABP, the CDF shows the amount of time spent below this level. Time is expressed as a percentage of the total number of (annotated) heartbeats recorded during surgery. Thus, the CDF revealed the distribution of SAP, MAP, and DAP over the time spent under anesthesia, not including bypass.

Figure 4-4 compares the CDFs for SAP and MAP for all patients. The graph of the SAP data (Figure 4-4a) shows that over half of the cases clustered on the right side of the group. Close inspection of the individual traces reveals that patients who experienced adverse outcomes had systolic values above 120 mmHg for over 50% of time spent under anesthesia. The distribution for MAP (Figure 4-4b) illustrates that at the hypotensive end of the distributions, there is a clear difference between cases and controls, suggesting that cases tended to be more hypotensive during surgery. This difference is even more obvious in Figure 4-5, where the DAP for patients who experienced adverse outcomes tends to be lower than for patients in the control group. Specifically, over 50% of the values recorded for DAP for patients in the case group are below 70 mmHg. Thus, in accordance with the literature, our initial results demonstrated that patients who experienced adverse outcomes spent more time outside a range of 70-120 mmHg than patients in the control group [1]. Furthermore, our results supported the finding that hypotension during bypass surgery can be an indicator of adverse events [15]. In summary, the review of the CDF for SAP, MAP, and DAP, yielded encouraging initial results and prompted a more in-depth analysis of the

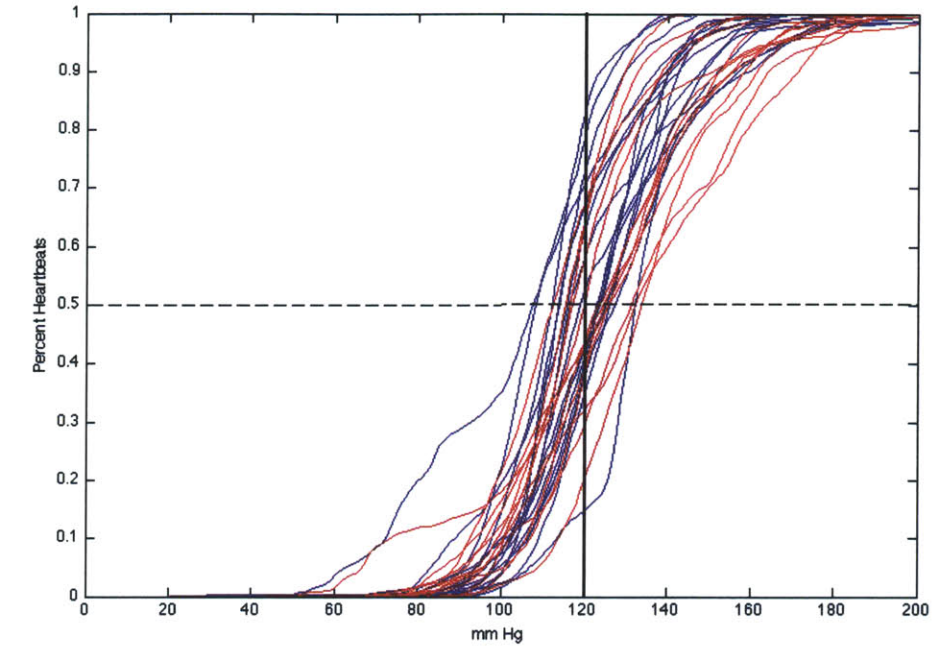

(a)

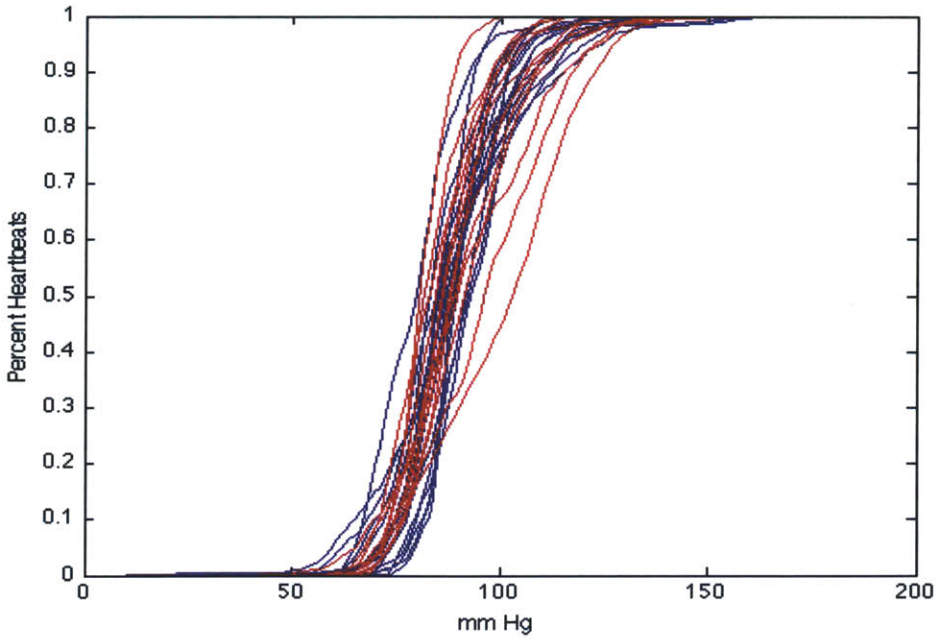

(b)

Figure 4-4: Cumulative distribution function for (a) SAP and (b) MAP in terms of percent heartbeats spent below a threshold pressure. Patients who experienced major adverse events (cases) are in red; control patients are in blue.

data extracted from the intraoperative ABP signals.

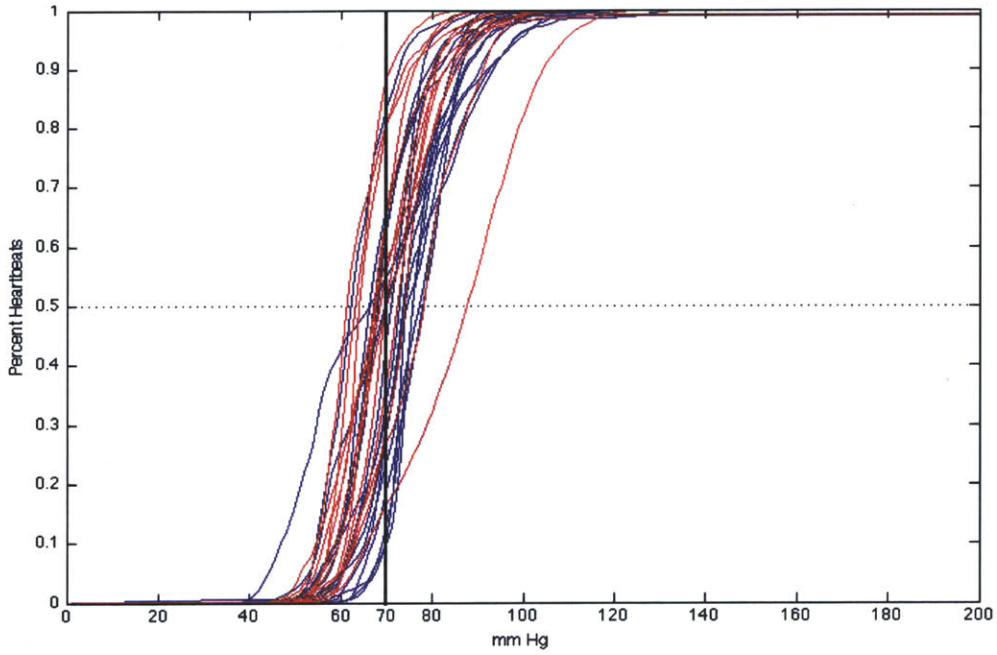

Figure 4-5: Cumulative distribution function for DAP in terms of percent heartbeats spent below a threshold value. Patients who experienced major adverse events (cases) are in red; control patients are in blue. The threshold pressure of 70 mmHg is marked by the vertical line; over 50% of diastolic values for cases were below this threshold whereas the diastolic values for those in the control group were generally above this value.

4.3 Cardiac Output and Total Peripheral Resistance Estimators

To further investigate possible differences in hemodynamics for the two patient groups, rough estimates for CO and TPR were calculated from the patient data using CO = HR×PP and TPR = $\frac{\text{MAP}}{\text{CO}}$. This estimate is derived from the Windkessel Model using Equations 3.7 and 3.6. Figure 4-6 shows this time series along with the time series of other hemodynamic variables for two representative patients (one from each group). Comparing the continuous signals for TPR, CO, and PP alongside the extracted signals for SAP, DAP, and HR helped visualize when certain factors were more influential. For instance, in Figure 4-6a, the pre-bypass CO waveform follows the PP waveform almost to the time of bypass, when HR rises and noticeably increases CO. Similarly, for Figure 4-6b, the variability of the PP throughout

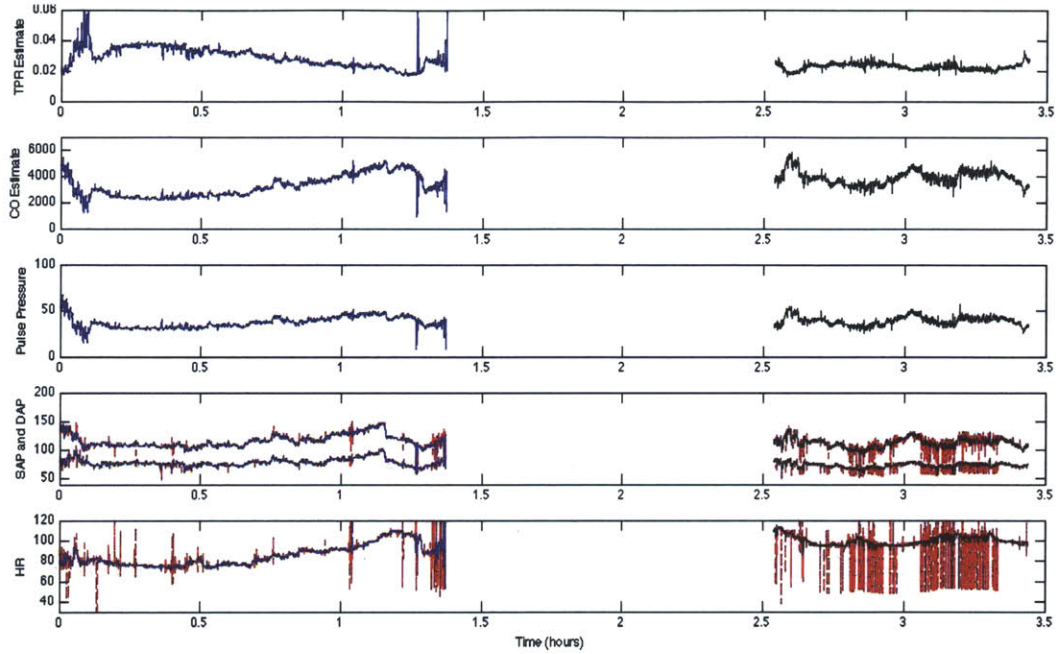

(a)

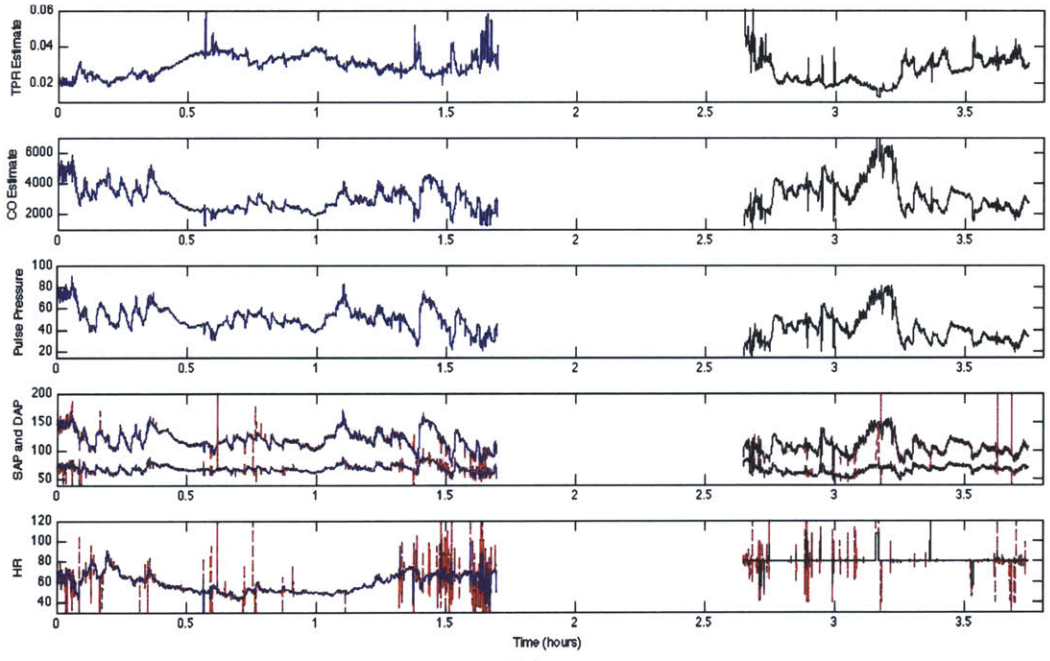

(b)

Figure 4-6: From bottom to top: HR, SAP, DAP, PP, CO, and TPR plots versus time for (a) a representative patient in the control group and (b) a representative patient in the case group during cardiothoracic surgery. The red signals in the bottom two plots of each figure are the unfiltered signals as they were extracted from the ABP data. The blue segments correspond to pre-bypass and black correspond to post-bypass. The gap between the two is the time spent under bypass.

surgery correspondingly affects the variability of the CO signal. Although these estimates were helpful in visualizing the signals, they yielded no further insight in distinguishing patients in the two groups from each other.

As discussed in Chapter 3, there are many methods for estimating CO from an ABP waveform. We used these methods to obtain alternative (uncalibrated) estimates of CO. These CO estimators are summarized in Table 4.1, and a comparison of these methods for two representative patients from our database is visualized in Figure 4-7. Unfortunately, CO values taken during surgery (using thermodilution) were not recorded, so the estimates could not be calibrated. In order to compare the dynamic variation in these estimates, we subtracted the mean and divided by the standard deviation for each estimate, yielding signals centered at zero. The comparison of estimators in Figure 4-7 showed that they produced very similar trends for CO. Because our estimates were uncalibrated, we could only compare CO variability as opposed to absolute values for each patient, and thus were unable to glean further information that could help differentiate patients in the two groups from each other or provide insight into the difference between blood pressure values for patients in the two groups.

Table 4.1: Summary of CO estimators (not calibrated).

Method	**CO Estimate**
Parlikar *et al.* [14]	$\frac{\Delta P_n}{T} + \frac{MAP}{\tau}$
Herd	$HR \cdot (MAP - DAP)$
Liljestrand & Zander	$HR \cdot \frac{SAP-DAP}{MAP+DAP}$
Liljestrand & Zander II	$HR \cdot \frac{MAP-DAP}{SAP+DAP}$
Rough Estimate (MAP)	$HR \cdot MAP$
Windkessel Estimate (PP)	$HR \cdot PP$
Windkessel Estimate (τ)	$\frac{MAP}{\tau}$

As part of the comparative analysis of CO estimators, TPR was derived from the CO estimates using $\text{TPR} = \frac{\text{MAP}}{\text{CO}}$. The purpose of comparing the obtained TPR signal was twofold; it was part of the initial investigation into patient hemodynamics during surgery, and served as a way to assess possible uses for CO estimators. Figure 4-8 gives a comparison of TPR estimators for a representative patient from each group. As was the case for CO, our estimates were uncalibrated, preventing comparison of values between patients. To compare

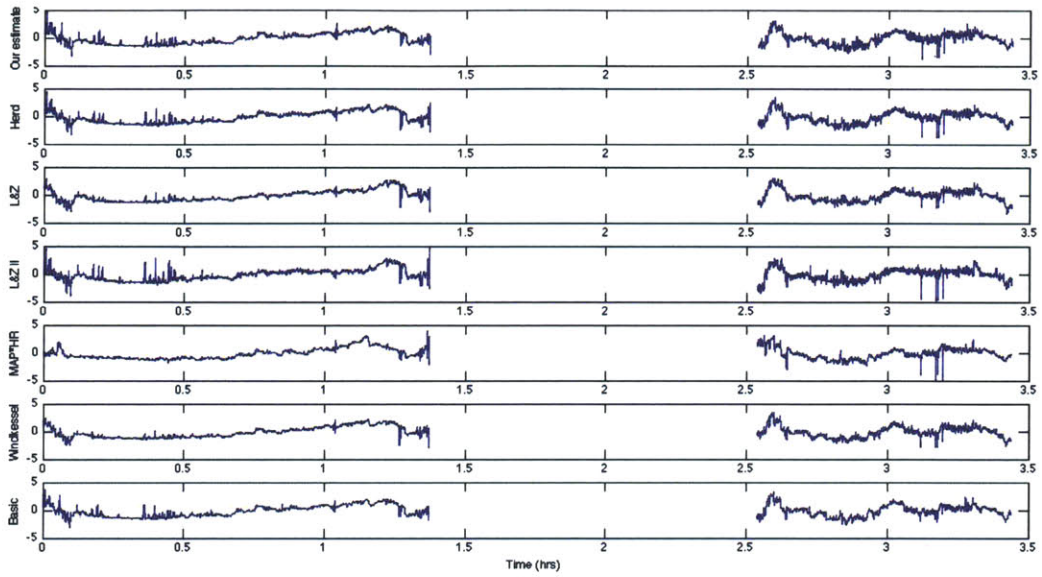

(a)

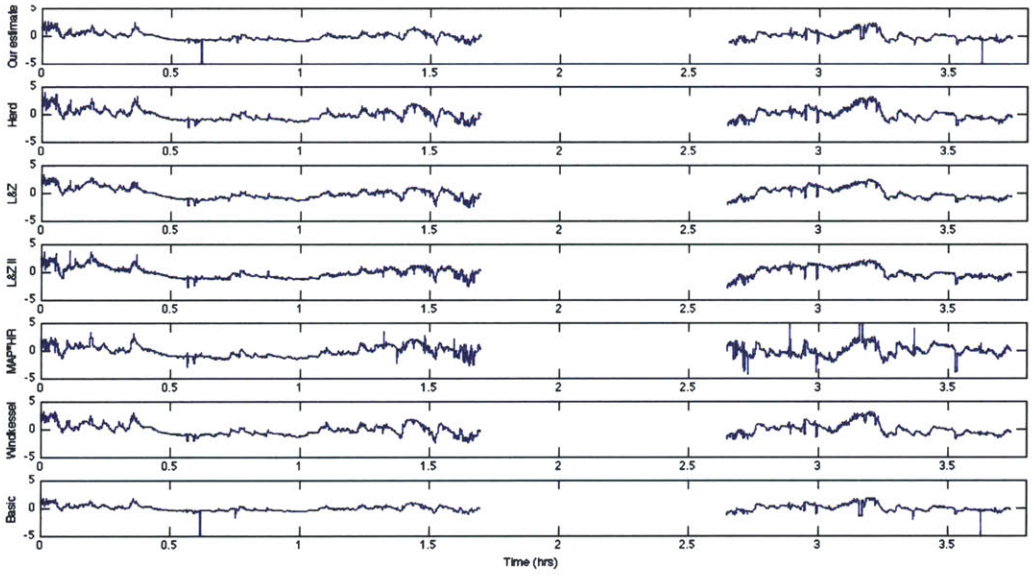

(b)

Figure 4-7: Comparison of CO Estimators for (a) a patient in the control group and (b) a patient in the case group. Algorithms used to derive CO from bottom to top: an estimate from the Windkessel model (using τ), the basic estimate using the Windkessel model, a rough estimate using MAP instead of PP, two versions based on the Liljestrand and Zander model, the Herd estimate, and the method by Parlikar *et al* [14].

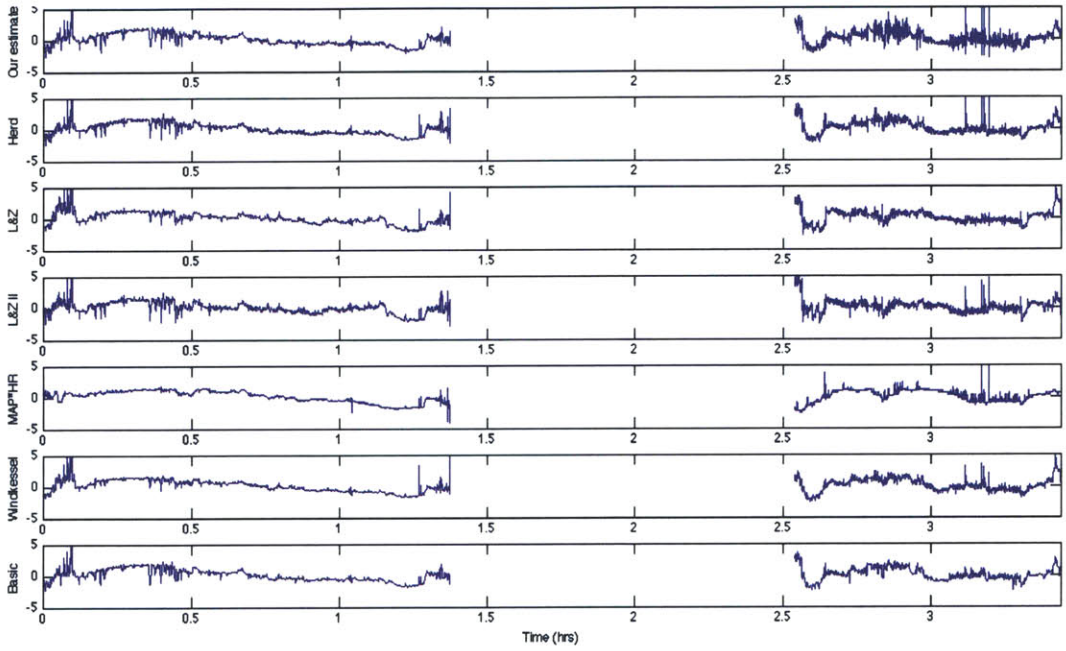

(a)

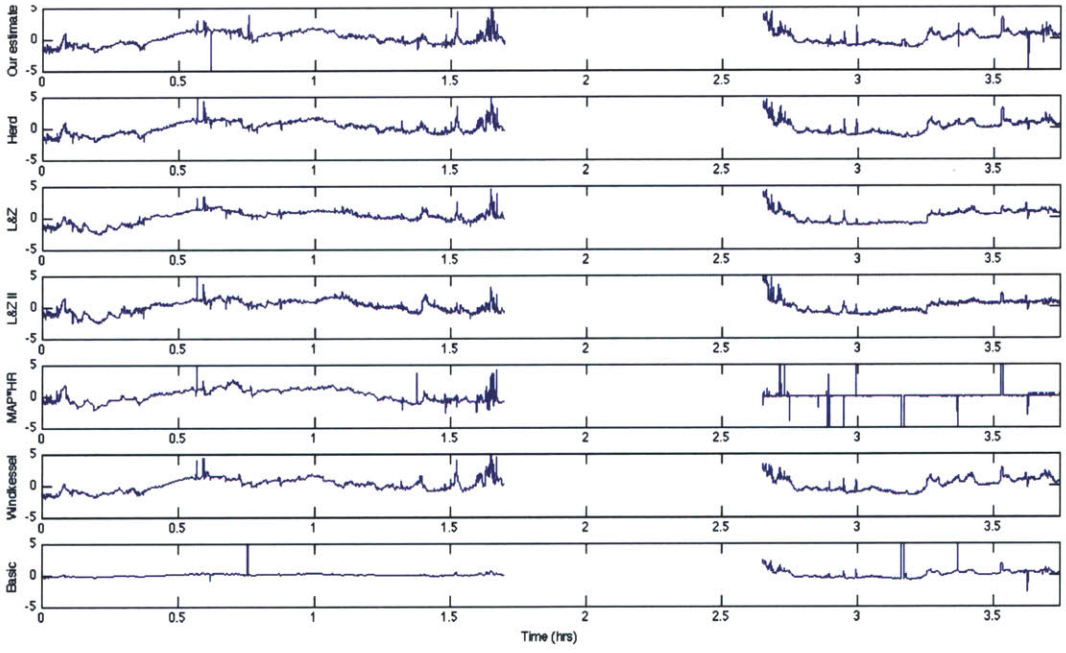

(b)

Figure 4-8: Comparison of TPR derived from CO estimates for (a) a patient in the control group and (b) a patient in the case group. Each TPR estimate was derived from the corresponding CO estimate in Figure 4-7.

estimators, we subtracted out the mean and divided each by its standard deviation but noted no substantial difference in the estimators.

Initially, it seemed that there was more variability in the hemodynamics for patients who experienced adverse outcomes after surgery. Using the CO estimate derived by Parlikar *et al.* [14] to estimate CO and then derive TPR, we compared the normalized variability, defined as the standard deviation divided by the mean, for pre-bypass and post-bypass hemodynamics for each patient. Figure 4-9 shows the comparison, illustrating that there was neither a difference in variability between the two groups nor in pre-bypass and post-bypass segments of surgery. However, although the data acquired in the CO and TPR estimator analysis ultimately did not help differentiate between patients in the two groups, having those signals visible during surgery could help connect certain events, such as procedures, or the administration of drugs and fluids, with changes in CO and TPR.

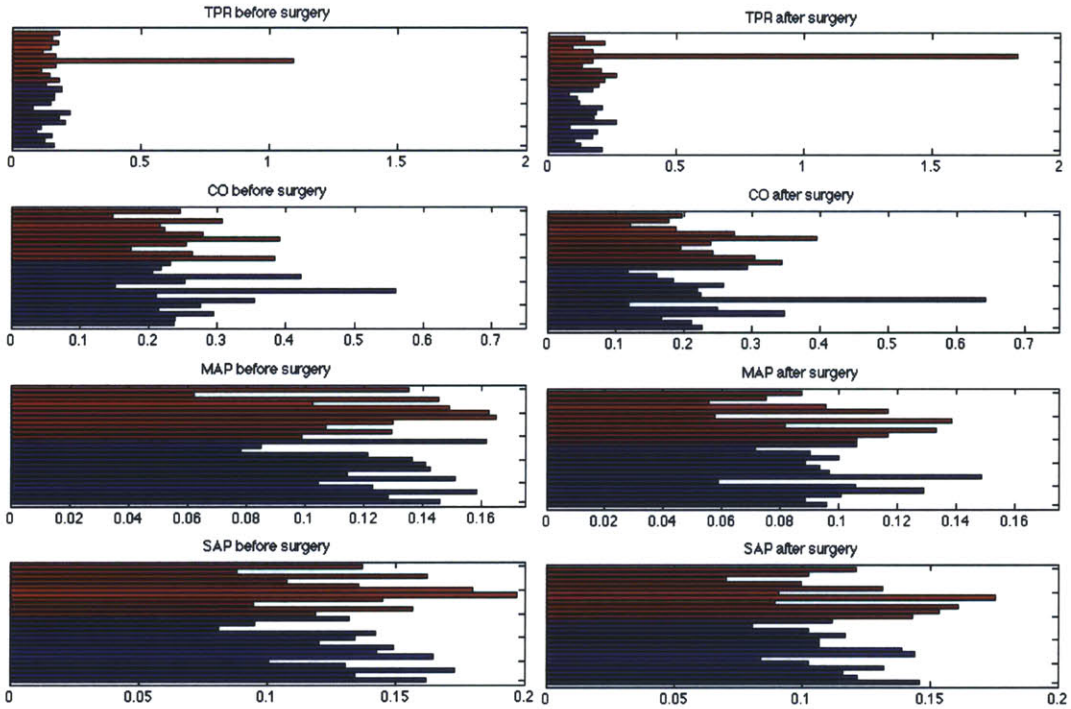

Figure 4-9: Comparison of normalized variability in (from bottom to top) SAP, MAP, CO, and TPR for each patient's (a) pre-bypass and (b) post-bypass segments. Patients who experienced major adverse events (cases) are in red; control patients are in blue.

4.4 Pulse Pressure Variability

An analysis of CO, and thus SV, can also aid in understanding other physiological features. For instance, Chapter 2 discussed the use of pulse pressure variability (PPV) in determining fluid responsiveness in mechanically ventilated patients. Thus, we can integrate our analysis of the data derived from the ABP waveform with other information collected during surgery, such as fluids administered for volume expansion. Patients who experienced adverse outcomes after surgery might respond differently to volume expansion. PPV has been suggested as a predictor of fluid responsiveness [12]. Therefore, an analysis of PPV and fluid administration during surgery could provide information differentiating the control group from the group of cases.

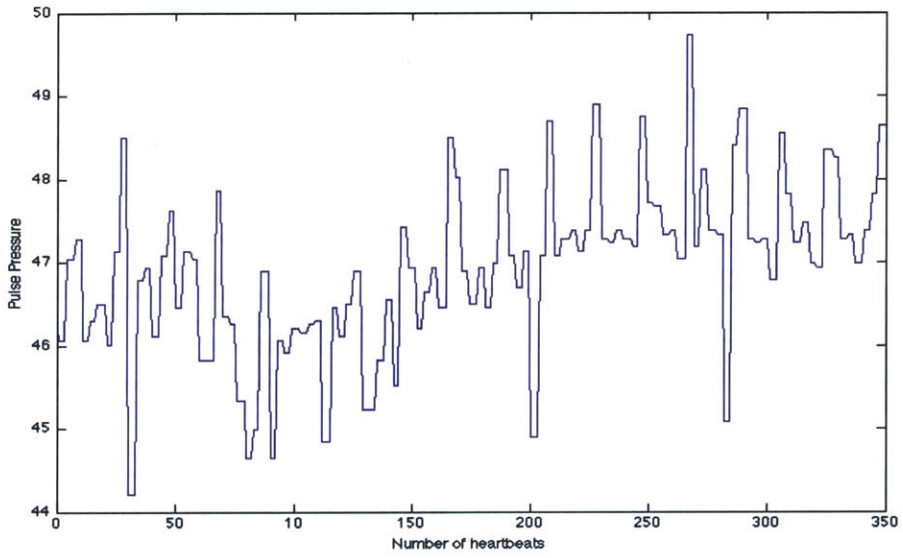

Figure 4-10: Pulse pressure time series displayed as a sample-and-hold waveform.

Pulse pressure variability is obtained from the pulse pressure time series. The original ABP signal recorded during surgery was sampled at 125 Hz to get the beat-by-beat numerics for SAP, MAP, DAP, and HR. Taking the difference between the extracted SAP and DAP signals gave a PP time series sampled at 125 Hz. We resampled the PP time series at 3 Hz since PP variations occur at respiratory frequencies. The subsequent PP waveform was a sample-and-hold waveform in which the length of each step was equal to the length of the

corresponding heartbeat (see Figure 4-10). As described in Chapter 2, PPV is calculated from the maximum and minimum values for PP over each respiratory cycle. Thus, it is necessary to first find the respiration frequency. Although patients were mechanically ventilated, we did not have access to the respiration waveforms, making it necessary to extract the respiration frequency from the PP (or other) time series. The respiration rate was found by taking the power spectral density (PSD) of the PP time series and analyzing PP fluctuations in the frequency domain. Figure 4-11 shows the PSD of the PP time series, with the DC value (PP mean) taken out. According to the surgery notes, respiration frequency was always set to a value between 8 and 12 breaths per minute, so a high-pass Butterworth filter was applied to the PP time series in order to focus on frequencies from 0.1 to 0.3 Hz (corresponding to a range of 6-18 breaths per minute). The next step in this analysis would be to obtain respiration frequency by detecting the dominant peak in this frequency range and normalizing it by the area under the PSD (or the sum of the squares of the PP time series). PPV is then calculated by applying a sliding window the length of the respiratory period to the PP waveform, extracting PP_{max} and PP_{min} for each iteration and using Equation 2.6 to calculate PPV for each window.

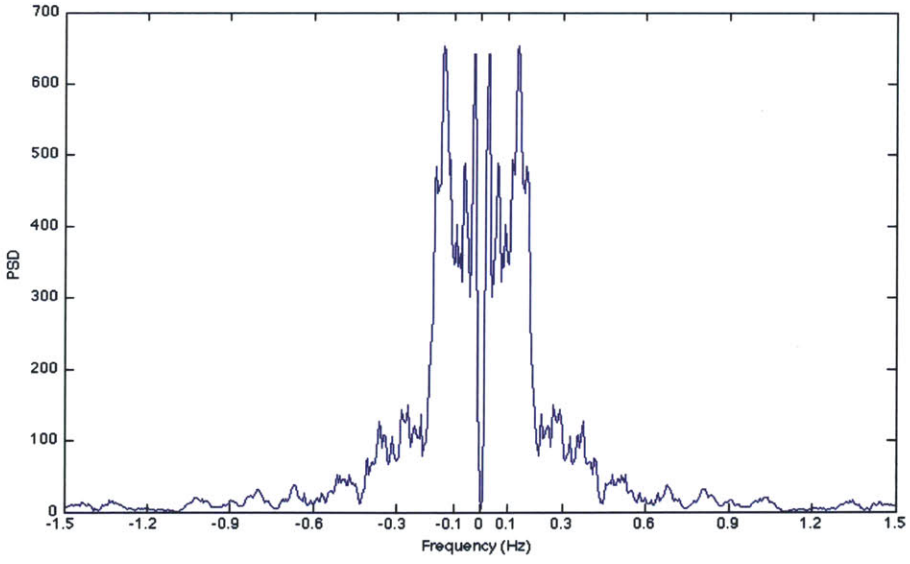

Figure 4-11: PSD of the PP time series shown in Figure 4-10. The peak corresponding to the respiratory frequency should be in the range of 0.1-0.3 Hz, corresponding to 6-18 breaths per minute.

Further analysis of PPV could involve annotating the PP time series waveform with the data for fluid administration to identify shifts in PP caused by volume expansion. Tying this information in with the values obtained for PPV would not only integrate data from a variety of sources in the OR (drug record, anesthesiology record, blood pressure) but also provide surgeons and anesthesiologists with useful information about a patient's state.

Chapter 5

Conclusions and Future Work

5.1 Summary

In this thesis, we have investigated possible differentiators between patients who experienced adverse outcomes after cardiothoracic surgery and those who did not. We analyzed the hemodynamics of 30 patients in order to gain further insight into blood pressure variability during surgery. Our exploratory analysis on the signals extracted directly from patient ABP data during surgery revealed a difference in the systolic and diastolic blood pressure signals between patients in the group of cases and patients in the control group. However, a comparative analysis of CO and TPR, using the estimators described in Chapter 3, yielded no clues to this difference. We concluded by documenting the initial steps taken towards analyzing patient PPV in order to investigate fluid responsiveness. The next section details where a continuation of that process could lead.

5.2 Future Work

Patient Data Set Much of the work behind this exploratory research was in integrating the data from multiple sources, limiting the number of patients analyzed. In particular, a lot of time of time was spent extracting the medication information from the surgery reports and displaying them alongside the hemodynamic data along a common time axis. A more extensive analysis would involve a larger and more diverse group, and could possibly show more definitive trends. Furthermore, the addition of more data could reveal trends for certain groups within the data set.

Cardiac Output and Total Peripheral Resistance Further analysis can be done by calibrating the CO estimates, allowing direct comparison of CO for patients in the two groups. Because the thermodilution measurements taken during surgery were not recorded, we were unable to do this, instead focusing on the normalized variability of CO and TPR for patients in the two groups. However, using patient records in which this information is saved would allow for a direct comparison of values for CO and thus TPR, possibly yielding further insight in our analysis of patient hemodynamics.

Pulse Pressure Variability Because we did not complete our assessment of PPV, future work would continue the process to calculate the PPV and identify possible trends or differences between the two patient groups. The analysis would be enhanced by the fact that we have records of fluids administered during surgery, allowing an investigation of fluid responsiveness in patients undergoing cardiothoracic surgery. By using PPV as a lens to examine fluid responsiveness, we could tie in this exploration with the CO and TPR data, leading to a more complete study of the hemodynamics in these patients.

Bibliography

[1] S. Aronson, M. Stafford-Smith, B. Phillips-Bute, A. Shaw, J. Gaca, and M. Newman. "Intraoperative systolic blood pressure variability predicts 30-day mortality in aorto-coronary bypass surgery patients". *Anesthesiology*, 113(2):305–12, August 2010.

[2] J.C. Chen. "A target for perioperative blood pressure during cardiac operation". *The Annals of Thoracic Surgery*, 89(2):672–3, 2010.

[3] L. S. Costanzo. *Physiology*, Chapter 4. Saunders, Philadelphia, Pennsylvania, fourth edition, 2010.

[4] O. Frank. "Die Grundform des arteriellen Pulses. Erste Abhandlung. Mathematische Analyse. *Zeitschrift für Biologie*, 37:485–526, 1899.

[5] A. L. Goldberger, L. A. N. Amaral, L. Glass, J. M. Hausdorff, P. Ch. Ivanov, R. G. Mark, J. E. Mietus, G. B. Moody, C.-K. Peng, and H. E. Stanley. "PhysioBank, PhysioToolkit, and PhysioNet: Components of a new research resource for complex physiologic signals". *Circulation*, 101(23):e215–e220, 2000 (June 13). Circulation Electronic Pages: http://circ.ahajournals.org/cgi/content/full/101/23/e215.

[6] A.C. Guyton and J.E. Hall. *Textbook of Medical Physiology.* Elsevier Saunders, Philadelphia, Pennsylvania, 12th edition, 2011.

[7] J. Herd, N. Leclair, and W. Simon. "Arterial pressure pulse contours during hemorrhage in anesthetized dogs". *Journal of Applied Physiology*, 21(6):1864–8, 1966.

[8] G. Liljestrand and E. Zander. "Vergleichende Bestimmung des Minutenvolumens des Herzens beim Menschen mittels der Sickoxydulmethode und durch Blutdruckmessung". *Z. Exp. Med.*, 59:105–22, 1928.

[9] P.E. Marik, R. Cavallazzi, T. Vasu, and A. Hirani. "Dynamic changes in arterial waveform derived variables and fluid responsiveness in mechanically ventilated patients: A systematic review of the literature". *Critical Care Medicine*, 37(9):2642–7, September 2009.

[10] R. G. Mark. 6.022J Course Notes: Cardiovascular mechanics I,II. MIT Open Courseware, Cambridge, Massachusetts, 2004. http://ocw.mit.edu/courses/health-sciences-and-technology/hst-542j-quantitative-physiology-organ-transport-systems-spring-2004/.

[11] F. Michard. "Changes in arterial pressure during mechanical ventilation". *Anesthesiology*, 103(2):419–28, 2005.

[12] F. Michard and J-L. Taboul. "Using heart-lung interactions to assess fluid responsiveness during mechanical ventilation". *Critical Care*, 4(5):282–9, September 2000.

[13] T.A. Parlikar. *Modeling and Monitoring of Cardiovascular Dynamics for Patients in Critical Care.* PhD dissertation, Massachusetts Institute of Technology, Department of Electrical Engineering and Computer Science, June 2007.

[14] T.A. Parlikar, T. Heldt, G.V. Ranade, and G.C. Verghese. "Model-based estimation of cardiac output and total peripheral resistance". *Computers in Cardiology*, 34:379–82, 2007.

[15] D.L. Reich, C.A. Bodian, M. Krol, M. Kuroda, T. Osinski, and D.M. Thys. "Intraoperative hemodynamic predictors of mortality, stroke, and myocardial infarction after coronary artery bypass surgery". *Anesthesia and Analgesia*, 89(4):814–22, 1999.

[16] K. Sagawa, R.K. Lie, and J. Schaefer. "Translation of Otto Frank's paper 'Die Grundform des arteriellen Pulses' ". *Journal of Molecular and Cellular Cardiology*, 22:253–77, 1990.

[17] J. X. Sun. Cardiac output estimation using arterial blood pressure waveforms. M.eng thesis, Massachusetts Institute of Technology, Department of Electrical Engineering and Computer Science, September 2006.

[18] W. Zong, T. Heldt, G. Moody, and R. Mark. "An open-source algorithm to detect onset of arterial blood pressure pulses". *Computers in Cardiology*, 30(9):259–62, 2003.

[19] W. Zong, G. Moody, and D. Jiang. "A robust open-source algorithm to detect onset and duration of QRS complexes". *Computers in Cardiology*, 30(9):737–40, 2003.